# Super-Resolution Ultrasound Localization Microscopy of Microvascular Structure and Flow for Distinguishing Metastatic Lymph Nodes – An Initial Human Study

## Lokalisierungsmikroskopie mit Superresolution-Ultraschall der mikrovaskulären Struktur und des Flusses zur Unterscheidung metastatischer Lymphknoten – eine erste Studie am Menschen

Authors

Jiaqi Zhu[1*], Chao Zhang[2*], Kirsten Christensen-Jeffries[3], Ge Zhang[1], Sevan Harput[4], Christopher Dunsby[5], Pintong Huang[2], Meng-Xing Tang[1]

Affiliations

1 Bioengineering, Imperial College London, London, United Kingdom of Great Britain and Northern Ireland
2 Department of Ultrasound, Zhejiang University School of Medicine Second Affiliated Hospital, Hangzhou, China
3 Imaging Sciences and Biomedical Engineering, King's College London School of Medical Education, London, United Kingdom of Great Britain and Northern Ireland
4 Division of Electrical and Electronic Engineering, London South Bank University, London, United Kingdom of Great Britain and Northern Ireland
5 Physics, Imperial College London, London, United Kingdom of Great Britain and Northern Ireland

Key words

blood flow, localization microscopy, microbubble contrast agents, super-resolution ultrasound, lymph node microvessel

**received** 08.09.2021
**accepted** 20.06.2022
**published online** 07.10.2022

Bibliography

Ultraschall in Med 2022; 43: 592–598
**DOI** 10.1055/a-1917-0016
**ISSN** 0172-4614

Georg Thieme Verlag KG, Rüdigerstraße 14, 70469 Stuttgart, Germany

Correspondence

Dr. Meng-Xing Tang
Imperial College London
Bioengineering, South Kensington Campus, SW7 2AZ London, United Kingdom of Great Britain and Northern Ireland
mengxing.tang@imperial.ac.uk

Prof. Pintong Huang
Department of Ultrasound, Second Affiliated Hospital, Zhejiang University School of Medicine, Hangzhou, People's Republic of China
huangpintong@zju.edu.cn

Additional material is available at https://doi.org/10.1055/a-1917-0016.

## ABSTRACT

**Purpose** Detecting and distinguishing metastatic lymph nodes (LNs) from those with benign lymphadenopathy are crucial for cancer diagnosis and prognosis but remain a clinical challenge. A recent advance in super-resolution ultrasound (SRUS) through localizing individual microbubbles has broken the diffraction limit and tracking enabled in vivo noninvasive imaging of vascular morphology and flow dynamics at a microscopic level. In this study we hypothesize that SRUS enables quantitative markers to distinguish metastatic LNs from benign ones in patients with lymphadenopathy.

**Materials and Methods** Clinical contrast-enhanced ultrasound image sequences of LNs from 6 patients with lymph node metastasis and 4 with benign lymphadenopathy were acquired and motion-corrected. These were then used to generate super-resolution microvascular images and super-resolved velocity maps. From these SRUS images, morphological and functional measures were obtained including microvessel density, fractal dimension, mean flow speed, and Local Flow Direction Irregularity (LFDI) measuring the variance in local flow direction. These measures were compared between pathologically proven reactive and metastasis LNs.

**Results** Our initial results indicate that the difference in the indicator of flow irregularity (LFDI) derived from the SRUS images is statistically significant between the two groups. The LFDI is 60 % higher in metastatic LNs compared with reactive nodes.

**Conclusion** This pilot study demonstrates the feasibility of super-resolution ultrasound for clinical imaging of lymph nodes

* These authors contributed equally.

and the potential of using the irregularity of local blood flow directions afforded by SRUS for the characterization of LNs.

ZUSAMMENFASSUNG

**Ziel** Der Nachweis und die Differenzierung metastatischer Lymphknoten (LK) von den LK einer benignen Lymphadenopathie sind entscheidend für die Krebsdiagnose und -prognose, stellen jedoch eine klinische Herausforderung dar. Ein neuer Fortschritt der Superresolution-Ultraschall-Bildgebung (SRUS) durch Lokalisierung einzelner Mikrobläschen hat die Beugungsgrenze durchbrochen und eine nicht invasive In-vivo-Bildgebung der Gefäßmorphologie und Flussdynamik auf mikroskopischer Ebene ermöglicht. In dieser Studie stellen wir die Hypothese auf, dass SRUS quantitativen Markern ermöglicht, metastatische von benignen LK bei Patienten mit Lymphadenopathie zu unterscheiden.

**Material und Methoden** Klinische kontrastverstärkte Ultraschall-Bildsequenzen der LK von 6 Patienten mit Lymphknoten-Metastasen und von 4 mit gutartiger Lymphadenopathie wurden aufgenommen und bewegungskorrigiert. Diese wurden dann verwendet, um hochaufgelöste mikrovaskuläre Bilder und hochaufgelöste Geschwindigkeitskarten zu erstellen. Aus diesen SRUS-Bildern wurden morphologische und funktionelle Messwerte gewonnen, darunter die Dichte der Mikrogefäße, die fraktale Dimension, die mittlere Flussgeschwindigkeit und die Unregelmäßigkeit der lokalen Flussrichtung („Local Flow Direction Irregularity“, LFDI), die die Abweichung der lokalen Flussrichtung misst. Diese Messungen wurden zwischen pathologisch nachgewiesenen reaktiven und metastatischen LK verglichen.

**Ergebnisse** Unsere ersten Ergebnisse deuten darauf hin, dass der Unterschied beim Indikator Fluss-Unregelmäßigkeit (LFDI), der aus den SRUS-Bildern abgeleitet wird, zwischen den beiden Gruppen statistisch signifikant ist. Die LFDI ist bei metastatischen LK um 60 % höher als bei reaktiven Knoten.

**Schlussfolgerung** Diese Pilotstudie zeigt die Durchführbarkeit der klinischen Superresolution-Ultraschall-Bildgebung bei Lymphknoten und das Potenzial der Nutzung der Unregelmäßigkeit lokaler Blutflussrichtungen, wie sie der SRUS für die Charakterisierung von LK bietet.

## Introduction

The lymph node (LN) is a key route for cancer metastasis and LN status is one of the most important indicators of prognosis in patients who are diagnosed with cancer. Currently, various modalities are used to characterize LNs, including ultrasound (US), magnetic resonance imaging (MRI), computed tomography (CT), and positron emission tomography (PET). Liao [1] has reported that the sensitivities of existing modalities US, MRI, CT, and PET for differentiating between benign and malignant LNs are low (< = 66 %). Invasive procedures such as LN dissection and excisional sentinel LN biopsy are routinely used for the diagnosis and management of cancer patients, despite the fact that many cancer patients do not have LN metastases at the time of diagnosis [2, 3]. Besides the cost of such invasive procedures, they can also cause complications like infection, lymphedema, and sensory loss [2, 4]. Hence, there is a pressing clinical need for an advanced noninvasive imaging modality to accurately characterize LN diseases.

Angiogenesis plays a fundamental role in the development of the chaotic and irregular vessel structure [5] and can contribute to the early detection, diagnosis, and prognosis of cancer [6]. From a physiological point of view, vessels whose function is of great significance for tissue integrity often lie at the perfusion level. Hence, noninvasive imaging of microvasculature can potentially address the aforementioned clinical need in LN characterization.

Contrast-enhanced ultrasound (CEUS) has emerged as a valuable tool for imaging flow and tissue perfusion in vivo [7]. CEUS has been used for imaging human lymph systems, e. g., for identifying sentinel LNs [8], and for distinguishing benign and malignant LNs [9]. However, due to various confounding factors in CEUS imaging [10], objective and quantitative clinical assessment of the images is challenging, and inconsistent results have been reported in different studies [11]. Furthermore, existing clinical CEUS has limited spatial resolution, making characterization of LNs (some < 1 cm) difficult.

Optical super-resolution has revolutionized the field of fluorescence microscopy [12]. Its acoustic counterpart, super-resolution ultrasound (SRUS), localizes and tracks individual microbubbles, enabling the quantification of microvascular structure and flow far beyond the wave diffraction resolution limit [13]. Notably, studies include the first demonstration of super-localization in vivo [14] and the first demonstration of super-resolution by separating two closely positioned structures as well as super-resolved velocity mapping [15, 16]. A number of following studies have demonstrated the feasibility of SRUS in vivo in animal models [17, 18, 19, 20, 21, 22] including tumor models [17, 21, 22], in healthy volunteers [23], and in breast cancer patients [21]. Recently phase change nanodroplets have also been used for real-time SRUS [24].

Volumetric SRUS images of LN vascular structure and flow dynamics have been demonstrated in a scanning 2D imaging approach on a rabbit model [19], offering a spatial resolution of < 30 microns. Noninvasive SRUS imaging with such resolution in deep tissue has great potential to improve the management of, e. g., cancer patients. However, the use of SRUS for human LN imaging to distinguish different pathologies has not been reported.

In this study we hypothesized that the application of SRUS imaging provides quantitative markers to distinguish metastatic LNs from benign (reactive) ones in patients with lymphadenopathy.

## Materials and methods

### Clinical data acquisition

CEUS data acquisition was performed on patients (**Supplementary Table 1**) with suspected lymphadenopathy between March

2019 and September 2019 at the Second Affiliated Hospital, Zhejiang University School Of Medicine. Ethical approval was provided by the University Institutional Ethics Board. Informed consent was signed by the participants before the ultrasound examination.

Ultrasound examinations were performed using a clinical scanner (Mindray Resona 7S) which provides live dual images of B-mode and CEUS. An L11–3U transducer was used with a transmit central frequency of 5.6 MHz. The patients were asked to breath normally. B-mode and color Doppler ultrasound was first used to identify the target node, and a long-axis view without a major artery nearby which otherwise can cause significant pulsatile motion. Then 1.2 ml SonoVue (Bracco, Milan, Italy) microbubbles were administered intravenously as a 2-second bolus followed by a flush of saline. Clinical CEUS data were acquired for at least 80 s after the injection, using a frame rate of 20 Hz in CEUS mode and a mechanical index (MI) of 0.085. The bubble concentration was adjusted by a flash sequence on the system at an MI of 0.553 at 40 s after injection, and a second flash was given if bubble concentration was judged high and individual bubbles could not be distinguished by visual assessment 60 s after injection. After CEUS acquisition, ultrasound-guided core needle biopsy was conducted according to the routine clinical management protocol. The pathological results received from biopsy were generated for comparison. The datasets for 10 out of 44 patients were included for producing SRUS images through post-processing of the CEUS images as they met the following conditions: (1) there is no large or significant out-of-plane motion; (2) the corresponding pathological diagnosis results were available; (3) the length of useable video data with appropriate bubble concentration was > = 30 s.

## Post-processing for SRUS image

SRUS images were obtained through off-line post-processing of the acquired video sequences.

After motion correction [23], an intensity threshold was estimated by maximum entropy to remove the noise. To detect microbubbles in the images, only regions with features including shape, intensity, and size that were inside the predefined ranges were accepted as a single microbubble signal. The ranges of these features were determined by the variations of individual bubble signals measured in a lab phantom using a similar ultrasound setting. These detected microbubbles were localized and tracked over frames and accumulated to generate SRUS images. Each centroid position of a detected microbubble was represented by a Gaussian profile in the localization density map with a standard deviation of 10 µm, given by the localization precision.

The tracking algorithm found the best correlated bubble signals within a search window between neighboring frames [13]. For each bubble signal identified in frame n, the intensity cross-correlation was calculated between that bubble and each of those bubbles found in frame n + 1 within a search window. The bubbles in different frames with the maximum normalized cross-correlation above an empirically determined threshold of 0.65 were paired. The search window size was defined according to the imaging frame rate and the maximum flow velocity of interest. Given the limited frame rate of 20 Hz for the clinical system, and as we were mainly interested in the micro-vessels where the flow velocity is typically several millimeters per second, 600 micrometers was set as the maximum search range so that flow velocities of up to 12 mm/s could be tracked.

The detected bubbles and tracks were accumulated to generate the SRUS images and flow velocity and direction maps. The SRUS processing pipeline is described in **supplementary Fig. S1**.

## Quantifications from super-resolution ultrasound image

### Vessel density

Vessel density is defined as the ratio of the total microvascular area in the binary LN SRUS microvascular map and the total area of the region of interest (ROI). The ROI is a manually selected full 2D cross-section of the LN. The binary SRUS microvascular map was generated by detecting the pixels in the SRUS map with an intensity higher than a localization threshold of 0.5.

### Vessel spatial complexity

Fractal dimension is a ratio providing a statistical index of complexity for a given structure/pattern. It is hypothesized that the microvascular structure associated with cancer would be more complex than that of normal tissue, and hence has a higher fractal dimension. The fractal dimension of the LN microvasculature was used to quantify the complexity of the microvascular geometry and estimated by applying the frequently used box-counting method developed by Russel et al. [25].

### Flow velocity and direction

Since microbubbles remain within the vascular space and have similar flow dynamics as red blood cells [26], the tracking of individual microbubbles was made to generate super-resolved maps of blood flow velocity and direction of the microvasculature.

### Local Flow Direction Irregularity (LFDI)

The blood flow in a malignant tumor is more likely to be disorganized. Therefore, a measure of how irregular local micro-flow is could be a promising marker for malignancy. This was only made possible by the high-resolution images of microvascular flow dynamics afforded by SRUS. We define Local Flow Direction Irregularity (LFDI) as the variance of flow direction within a defined local region/window:

$Var(angle) = E[(angle - E(angle))^2]$

where E denotes the mathematical expectation, and angle denotes the flow direction obtained through super-resolved velocity mapping. The LFDI was calculated block-by-block for each non-overlapping 2 mm × 2 mm block regions within the segmented LN ROI. A block size of 2 mm was defined according to the difference between micro-metastases (less than or equal to 2 mm) and macro-metastases (greater than 2 mm).

The mean and standard deviations of the different measures were generated from 4 reactive and 6 metastatic LN acquisitions. Student's two sample t-test was used to test the statistical significance of differences in the different image markers between metastatic and reactive LNs.

## Results

▶ **Fig. 1** shows B-mode, CEUS maximum intensity projection (MIP), and SRUS images of two sample LNs. The LN ROI is indicated by the green line.

**Supplementary Fig. S2** illustrates that SRUS image contains more detailed morphological information which is not visible in the MIP image. Figs. S2B and C show higher magnification of the same ROI from the MIP and SRUS velocity map. The same ROI is indicated with the white box in Fig. S2A.

**Supplementary Fig. S3** shows a comparison of a classic Doppler vascular image and the SRUS image of the same reactive LN. As can be seen in the color Doppler image, only major vessels with fast blood flow (up to 6.7 cm/s) are visualized. In the corresponding SRUS velocity map, blood flow with a much slower velocity can be detected.

Figs. 2A and 2C show the SRUS direction maps for the same two LNs as Fig 1. The corresponding LFDI maps are also visualized in Figs. 2B and 2 D. As can be seen from the figure, the reactive LN shown in ▶ **Fig. 2B** has a lower LFDI and appears more homogeneous than that of the metastatic LN shown in ▶ **Fig. 2D**.

▶ **Fig. 3** displays measurements of micro-vessel density, fractal dimension, mean velocity, and LFDI for the reactive and metastatic LNs. As can be seen, reactive LNs have a significantly lower LFDI (1000 ± 376) than that of metastatic LNs (1600 ± 388, P = 0.0465). While the estimated micro-vessel density has a lower average value (31 ± 10 %) in reactive LNs than in metastatic LNs (42 ± 5 %), no statistically significant difference was found. For the results of fractal dimension, reactive LNs have a similar value (1.75 ± 0.04) as that of metastatic LNs (1.79 ± 0.05). The measured blood flow velocity has a slightly higher average (2.0 ± 0.7) for reactive LNs than for metastatic LNs (1.8 ± 0.5), although the difference is again not statistically significant.

## Discussion

Abnormal hemodynamics in tumor-associated vasculature can be a valuable imaging marker clinically, but currently there is a lack of an effective tool to evaluate this in vivo in deep tissue. Since SRUS is able to generate a microvascular morphology and flow velocity map with resolution at the microscopic level, it allows the analysis of local hemodynamics in greater detail.

In this study we have, for the first time as far as we are aware, applied SRUS to the evaluation of LNs in patients with lymphadenopathy using a clinical scanner. An image marker derived from the SRUS flow maps, Local Flow Direction Irregularity (LFDI), shows a statistically significant difference between reactive and metastatic LNs, even at a very low sample number (10 patients in total). This is encouraging and consistent with our expectation of increased heterogeneity in hemodynamics in tumor-associated vasculature [27]. It should be noted that in Opacic [21] an entropy measure was used to characterize the local microvascular flow direction, similar to the LFDI measure presented in this study.

A number of other quantitative image markers derived from the SRUS images including micro-vessel density, micro-flow velocity, and vessel fractal dimension were also generated. As shown in ▶ **Fig. 3**, the estimated micro-vessel density has a lower average value in reactive LNs than in metastatic LNs. This is consistent with the positive correlation between micro-vessel density and tumor occurrence which have been reported in previous studies [28]. However, the difference is not statistically significant,

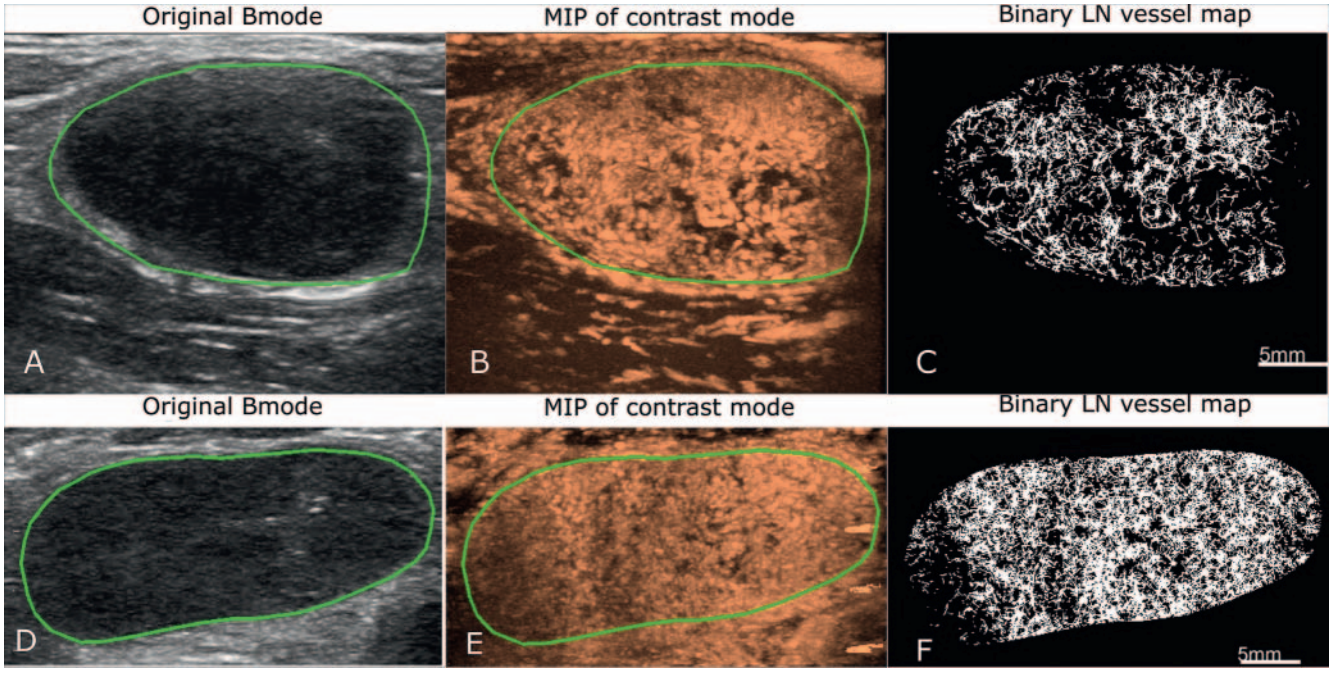


▶ **Fig. 1** Images of two sample LNs (**A, B, C** are from a reactive lymph node; **D, E, F** from a metastatic lymph node). **A, D**: Conventional B-mode ultrasound, LN region of interest (ROI) is manually segmented from the original B-mode image as indicated by the green contour. **B, E**: Maximum Intensity Projection (MIP) images of the LNs. **C, F**: Super-resolution binary LN vessel map.

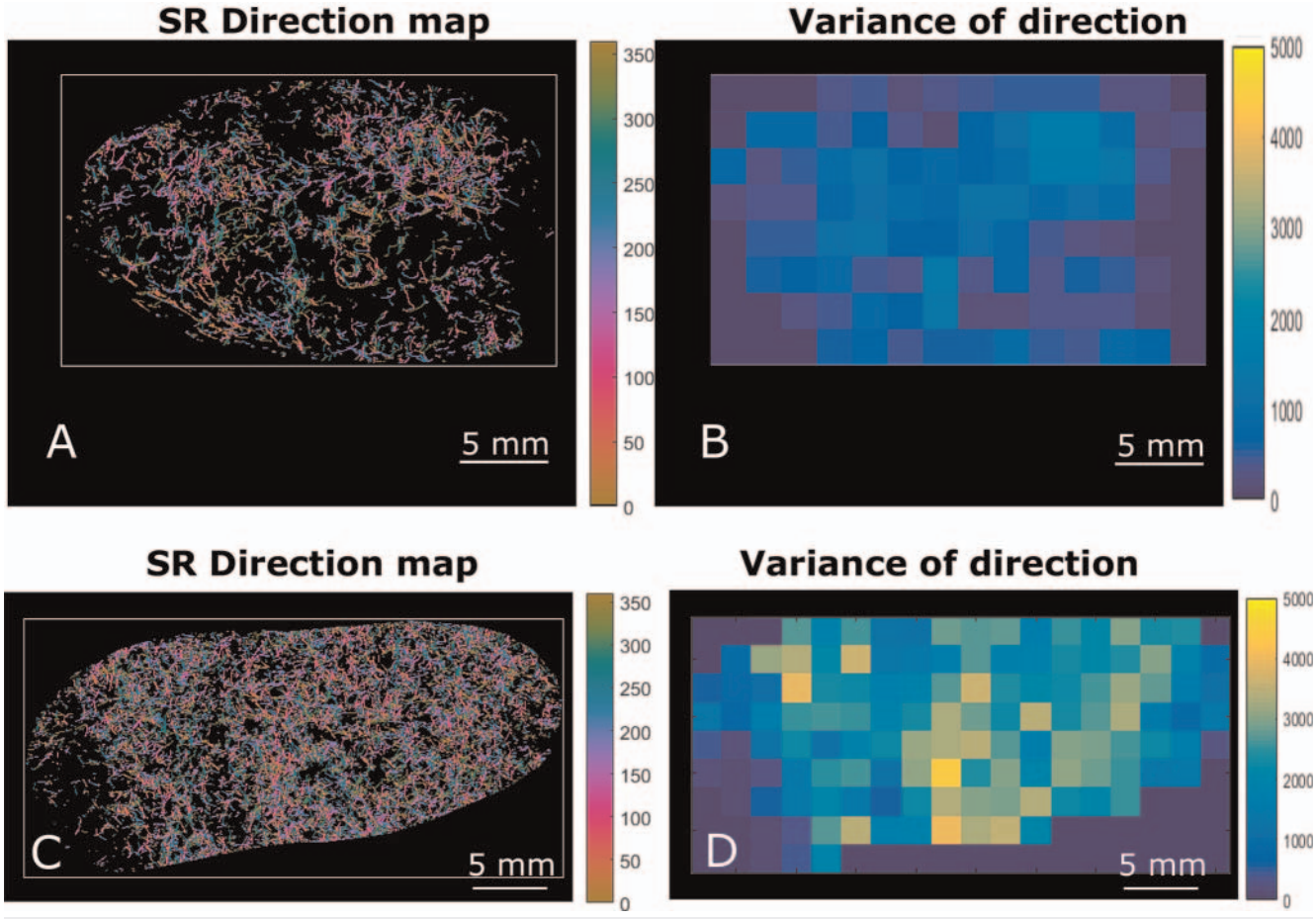


▶ **Fig. 2 A, C**: Super-resolution flow direction maps of two LNs, where color codes the angle of blood flow direction; **B, D**: Local Flow Direction Irregularity (LFDI) maps show a higher degree of irregularity in the metastatic LN in **D** compared to the reactive LN in **B**.

likely due to the small number of samples and the different types of malignancies and locations of LNs used in this study. The data here contains five different types of malignancies from various body locations. Furthermore, the different time points since the onset of the cancer for each patient is also a confounding factor. This has increased the variability of the data within each group. Previous studies using spectral Doppler sonography have shown increased flow velocity in reactive LNs [29]. Furthermore, it was reported that the overall blood flow velocity tends to be lower in tumors than in normal tissues [30]. These are consistent with the data shown here.

SRUS imaging offers visualization and quantification of individual micro-vessels, not achievable in conventional modalities. These novel measures open new avenues for characterizing metastatic LNs in order to inform patient management. The gold-standard procedure for LN staging is still surgical excision and histopathological assessment, despite the fact that many patients with cancer do not have LN metastases at the time of surgery, and that the procedure can result in complications. Our results demonstrate that SRUS as a noninvasive imaging modality has potential to assist LN diagnosis. 2 D imaging with a single slice of an LN which is a 3 D structure certainly poses a risk of missing a micro-metastasis. Multiple 2 D slice acquisitions would reduce such a risk, but this will reduce the time spent on each acquisition given the limited persistence of the bubble signals in vivo, and as a result the number of localizations and signal-to-noise ratio for each individual 2 D SRUS image may be reduced. However, given that SRUS imaging requires low bubble concentration, it is possible to change from a bolus to an infusion so that a sufficient amount of data from multiple planes can be acquired. Further clinical studies should be done to optimize data acquisition for multiple 2D slices.

One limitation of this study is the low number of patients. In this study out of the 44 patient datasets, 34 were not used for SRUS processing, mainly due to out-of-plane or large motion (14 datasets), and also due to the usable video length with appropriate bubble concentration being less than 30 s (20 datasets). The data acquisition protocol should be further optimized. A slightly longer acquisition time or acquisition at a later time after injection could generate data with more appropriate bubble concentration for SRUS. More training for operators as well as future full 3D imaging technologies would help address the out-of-plane motion issue. Further development of more advanced post-processing would also help to make use of data with higher bubble concentrations and greater motion.

Another limitation of the study is that the super-resolved flow velocity tracking is limited to a flow velocity of ~12 mm/s or less.

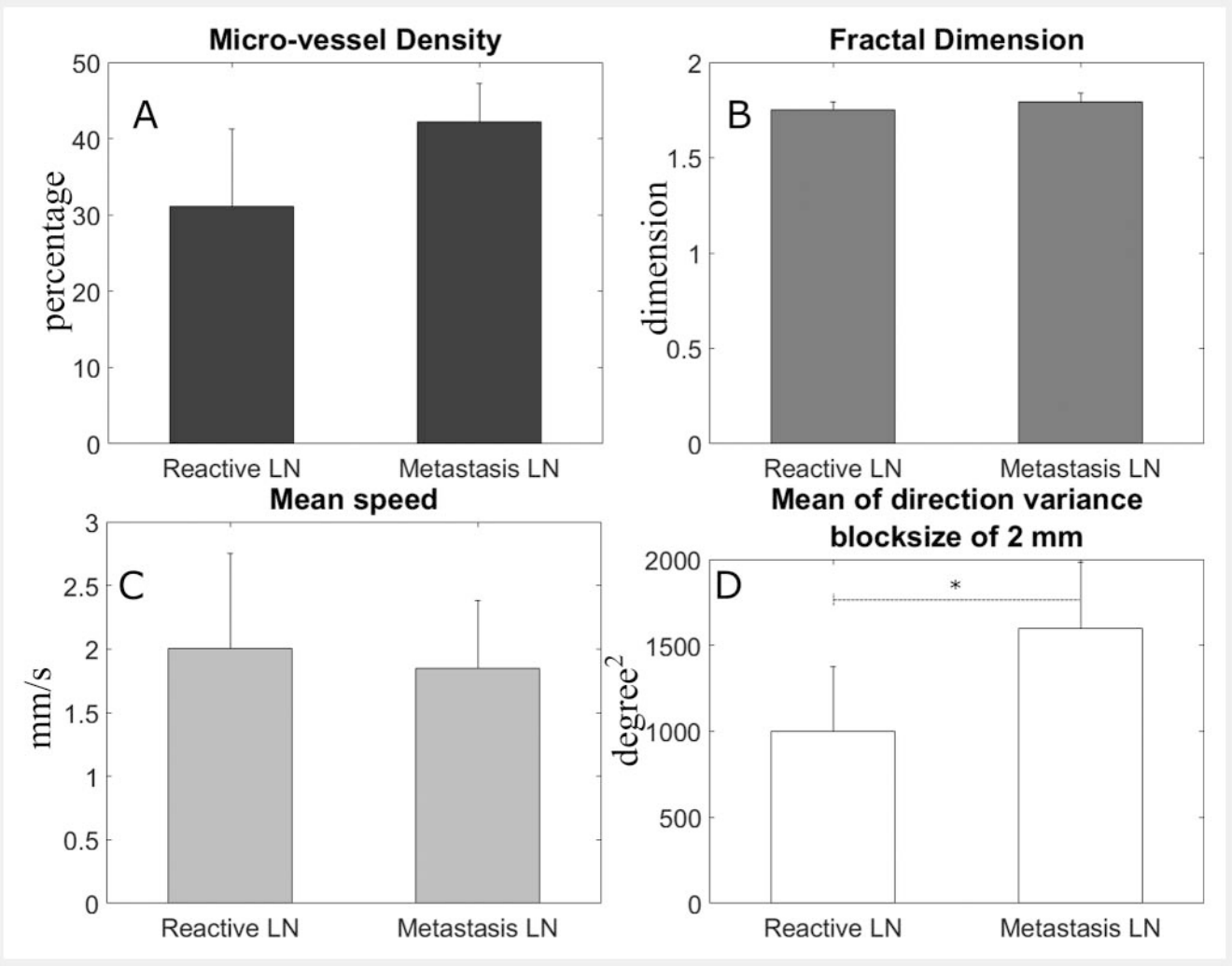


▶ **Fig. 3** Quantification results in reactive (n = 4) and metastasis (n = 6) LNs: **A**: micro-vessel density. **B**: fractal dimension. **C**: mean speed and **D**: Local Flow Direction Irregularity (LFDI). Significant difference between reactive and metastatic LNs was only found in the LFDI ($P < 0.05$.).

This is primarily due to the limited imaging frame rate available to the clinical system being used. A higher frame rate system will allow flows in a broader range to be tracked. Additionally, while the flow velocities were calculated based on bubble pairs in this study, velocity estimation using the Kalman filter based on multiple frames [21] may provide a more robust estimation. A further limitation of this study is that while we have clinical diagnosis of the LNs in this study through core needle biopsy and pathology as part of the patients' clinical management, we do not have sufficient information to be able to generate a spatial correspondence between the pathology and the SRUS images.

## Conclusion

In this study we have, for the first time as far as we are aware, applied SRUS to the evaluation of LNs in patients with lymphadenopathy. Local microvascular flow direction irregularity has been shown to be a promising marker for distinguishing metastatic LNs.


## Funding

Engineering and Physical Sciences Research Council | http://dx.doi.org/10.13039/501100000266 (EP/N015487/1) | NIHR (NIHR200972) | Cancer Research UK | http://dx.doi.org/10.13039/501100000289 (C53470/A22353)


## Conflict of Interest

MT declares that they have received lecture fees from Bracco, and is a stake holder of Sonalis.

## References


[1] Liao LJ, Lo WC, Hsu WL et al. 'Detection of cervical lymph node metastasis in head and neck cancer patients with clinically N0 neck – a meta-analysis comparing different imaging modalities'. BMC Cancer 2012; 12: 236

[2] Krag DN et al. 'Sentinel-lymph-node resection compared with conventional axillary-lymph-node dissection in clinically node-negative patients with breast cancer: overall survival findings from the NSABP B-32 randomised phase 3 trial'. Lancet Oncol 2010; 10 (11): 927–933

[3] Li N, Cui M, Yu P et al. Correlations of lncRNAs with cervical lymph node metastasis and prognosis of papillary thyroid carcinoma. Onco Targets Ther 2019; 12: 1269–1278. doi:10.2147/OTT.S191700

[4] Mansel RE et al. 'Randomized Multicenter Trial of Sentinel Node Biopsy Versus Standard Axillary Treatment in Operable Breast Cancer: The ALMANAC Trial', JNCI J. Natl. Cancer Inst 2006; 98 (9): 599–609. doi:10.1093/jnci/djj158

[5] Carmeliet P, Jain R. Angiogenesis in cancer and other diseases. Nature 2000; 407: 249–257. doi:10.1038/35025220

[6] Farnsworth R, Lackmann M, Achen M et al. Vascular remodeling in cancer. Oncogene 2014; 33: 3496–3505. doi:10.1038/onc.2013.304

[7] Lindner JR. "Microbubbles in medical imaging: current applications and future directions". Nature Reviews Drug Discovery 2004; 3 (6): 527–532. doi:10.1038/nrd1417

[8] Sever A, Jones S, Cox K et al. Preoperative localization of sentinel lymph nodes using intradermal microbubbles and contrast-enhanced ultrasonography in patients with breast cancer. Br J Surg 2009; 96: 1295–1299. doi:10.1002/bjs.6725

[9] Chen L, Chen L, Liu J et al. 'Value of Qualitative and Quantitative Contrast-Enhanced Ultrasound Analysis in Preoperative Diagnosis of Cervical Lymph Node Metastasis From Papillary Thyroid Carcinoma', J. Ultrasound Med. Off. J. Am. Inst. Ultrasound Med 2020; 39 (1): 73–81. doi:10.1002/jum.15074

[10] Tang MX et al. 'Quantitative contrast-enhanced ultrasound imaging: a review of sources of variability'. Interface Focus 2011; 04 (1): 520–539

[11] Dudau C et al. 'Can Contrast-Enhanced Ultrasound Distinguish Malignant from Reactive Lymph Nodes in Patients with Head and Neck Cancers?', Ultrasound Med. Biol 2014; 40 (4): 747–754. doi:10.1016/j.ultrasmedbio.2013.10.015

[12] Betzig E, Patterson GH, Sougrat R et al. Imaging intracellular fluorescent proteins at nanometer resolution. Science 2006; 313: 1642–1645. doi:10.1126/science.1127344

[13] Christensen-Jeffries K, Couture O, Dayton PA et al. Super-resolution Ultrasound Imaging. Ultrasound in Medicine & Biology 2020; 46 (4): 865–891. doi:10.1016/j.ultrasmedbio.2019.11.013

[14] Siepmann M, Schmitz G, Bzyl J et al. Imaging tumor vascularity by tracing single microbubbles. IEEE IUS 2011: 1906–1909

[15] Christensen-Jeffries K, Browning RJ, Tang MX et al. In vivo acoustic super-resolution and super-resolved velocity mapping using microbubbles. IEEE TMI 2015; 34: 433–440

[16] Errico C, Pierre J, Pezet S et al. Ultrafast ultrasound localization microscopy for deep super-resolution vascular imaging. Nature 2015; 527: 499. doi:10.1038/nature16066

[17] Lin F, Shelton SE, Espíndola D et al. 3-D ultrasound localization microscopy for identifying microvascular morphology features of tumor angiogenesis at a resolution beyond the diffraction limit of conventional ultrasound. Theranostics 2017; 7: 196

[18] Song P, Trzasko JD, Manduca A et al. Improved super-resolution ultrasound microvessel imaging with spatiotemporal nonlocal means filtering and bipartite graph-based microbubble tracking. IEEE T UFFC 2017; 65: 149–167

[19] Zhu J, Rowland EM, Harput S et al. 3D Super-Resolution US Imaging of Rabbit Lymph Node Vasculature in Vivo by Using Microbubbles. Radiology 2019; 291: 642–650. doi:10.1148/radiol.2019182593

[20] Kanoulas E, Butler M, Rowley C et al. Super-Resolution Contrast-Enhanced Ultrasound Methodology for the Identification of In Vivo Vascular Dynamics in 2D. Investigative Radiology 2019; 54 (8): 500–516. doi:10.1097/RLI.0000000000000565

[21] Opacic T, Dencks S, Theek B et al. Motion model ultrasound localization microscopy for preclinical and clinical multiparametric tumor characterization. Nature communications 2018; 9: 1527. doi:10.1038/s41467-018-03973-8

[22] Zhang W, Lowerison MR, Dong Z et al. Super-Resolution Ultrasound Localization Microscopy on a Rabbit Liver VX2 Tumor Model: An Initial Feasibility Study. Ultrasound Med Biol 2021; 47 (8): 2416–2429. doi:10.1016/j.ultrasmedbio.2021.04.012

[23] Harput S, Christensen-Jeffries K, Brown J et al. Two-Stage Motion Correction for Super-Resolution Ultrasound Imaging in Human Lower Limb. IEEE T UFFC 2018; 65: 803–814. doi:10.1109/TUFFC.2018.2824846

[24] Zhang G, Harput S, Hu H et al. « Fast Acoustic Wave Sparsely Activated Localization Microscopy: Ultrasound Super-Resolution Using Plane-Wave Activation of Nanodroplets ». IEEE T UFFC 2019; 66 (6): 1039–46

[25] Russell DA, Hanson JD, Ott E. 'Dimension of Strange Attractors'. Phys Rev Lett 1980; 45 (14): 1175–1178

[26] Suad I, Jayaweera Ananda R, Camarano G et al. 'Relation Between Air-Filled Albumin Microbubble and Red Blood Cell Rheology in the Human Myocardium'. Circulation 1996; 94 (3): 445–451

[27] Leunig M et al. 'Angiogenesis, Microvascular Architecture, Microhemodynamics, and Interstitial Fluid Pressure during Early Growth of Human Adenocarcinoma LS174T in SCID Mice'. Cancer Res 1992; 52 (23): 6553–6560

[28] Saad R, Kordunsky L, Liu Y et al. Lymphatic microvessel density as prognostic marker in colorectal cancer. Mod Pathol 2006; 19: 1317–1323. doi:10.1038/modpathol.3800651

[29] Ahuja AT, Ying M. 'Sonographic Evaluation of Cervical Lymph Nodes'. Am J Roentgenol 2005; 184 (5): 1691–1699

[30] Nagy JA, Chang SH, Dvorak AM et al. 'Why are tumour blood vessels abnormal and why is it important to know?'. Br J Cancer 2009; 100 (6): 865–869. doi:10.1038/sj.bjc.6604929